02

Analysis of fluctuation conductivity in $Y_{0.5}Cd_{0.5}Ba_2Cu_3O_{7-\delta}$

© V.M. Aliev [1], G.I. Isakov [2], J.A. Ragimov [1], R.I. Selim-zade [3], G.A. Alieva [1]

[1] Institute of Physics of the Ministry of Science and Education of Azerbaijan,
Baku, Azerbaijan
[2] Azerbaijan Medical University,
Baku, Azerbaijan
[3] Institute of National Arts of the Ministry of Science and Education of Azerbaijan,
Baku, Azerbaijan
E-mail: v_aliev@bk.ru

Received December 3, 2022
Revised December 22, 2022
Accepted December 28, 2022

A study was made of the influence of substitution of up to 50% of yttrium for cadmium in $YBa_2Cu_3O_{7-\delta}$ polycrystals on the mechanism of formation of excess conductivity. It has been established that such a substitution led to a significant increase in the resistivity of $Y_{0.5}Cd_{0.5}Ba_2Cu_3O_{7-\delta}$, and the value of the critical transition temperature T_c to the superconducting state decreases. The mechanism of formation of fluctuation conductivity (T) near Tc is considered within the framework of the Aslamazov–Larkin theory. The Ginzburg temperature, the critical temperature in the mean field approximation, and the 3D-2D crossover temperature were determined. It is shown that the doping of YBa $YBa_2Cu_3O_{7-\delta}$ with cadmium leads to an increase in the coherence length along the c axis by a factor of 3.2. An analysis of the excess conductivity of the $Y_{0.5}Cd_{0.5}Ba_2Cu_3O_{7-\delta}$ sample within the framework of the local pair model made it possible to determine the temperature dependences of the pseudogap and its maximum value.

Keywords: superconductivity, fluctuation conductivity, pseudo-gap, coherence length.

DOI: 10.21883/PSS.2023.03.55579.546

1. Introduction

The analysis of experimental results of charge transfer phenomena in metal oxide high temperature superconductors (HTSC) is complicated by a number of factors: complex crystal structure [1–3] inhomogeneous distribution of structural defects [4], opportunity of cluster formation and formation of grain boundaries [5]; heterogeneity of polycrystalline samples [6], due to the peculiarities of the technological processes of synthesis, etc.

For a number of HTSC compounds, in addition to the properties usual for superconductors, an interesting phenomenon is observed: in the normal phase of HTSC, a pseudogap (PG) opens in the excitation sector at a certain characteristic temperature $T^* \gg T_c$ (T_c — critical transition temperature into the superconducting state) [7–10]. Elucidation of the physics of PG formation inherent in cuprates [11,12] will allow to answer a number of questions about the mechanism of superconducting (SC) pairing in a HTSC.

One of the research directions of HTSC with CuO_2 active plane is the improvement of their SC characteristics due to isomorphic substitutions of one of the components [13–20]. From this point of view, the compound $YBa_2Cu_3O_{7-\delta}$ (YBCO) is attractive due to the opportunity of wide variation of the composition by replacing yttrium with its isoelectronic analogs, or by changing the degree of oxygen nonstoichiometry. Note that yttrium in the composition of YBCO is easily replaced by most lanthanides and other elements [1,21–30], which usually does not lead to deterioration of the SP properties of the initial composition. The exception is praseodymium, t.k. PrBCO — dielectric [31,32].

Earlier in [33] we analyzed the fluctuation conductivity in the compositions $Y_{1-x}Cd_xBa_2Cu_3O_{7-\delta}$ ($x = 0$–0.4). In the present work, the studies of the normal state of $YBa_2Cu_3O_{7-\delta}$ (Y1) and $Y_{0.5}Cd_{0.5}Ba_2Cu\ _3O_{7-\delta}$ (Y2) in the temperature range $T^* > T > T_c$, in order to determine their physical characteristics, as well as to identify the opportunity of the appearance of a PG state in the composition of $Y_{0.5}Cd_{0.5}Ba_2Cu_3O_{7-\delta}$. The analysis of the experimental results was carried out on the basis of identifying the excess conductivity above T_c as part of the model of local pairs (LP) [12,18,20] as part of the fluctuation theory of Aslamazov–Larkin (AL) and Hikami–Larkin (KhL) [34,35] near T_c. Near temperature T_c, the fluctuation conductivity (FLC) $\Delta\sigma(T)$ of samples Y1 and Y2 is well described by the three-dimensional (3D) equation of AL theory, which is typical for HTSC [1,11,32]. The temperature dependence of the pseudogap was analyzed as part of the local pair model developed in [11,36,37].

2. Experiment

Choice of the research object: The Y–Ba–Cu–O HTSC material with the substitution of yttrium for cadmium was

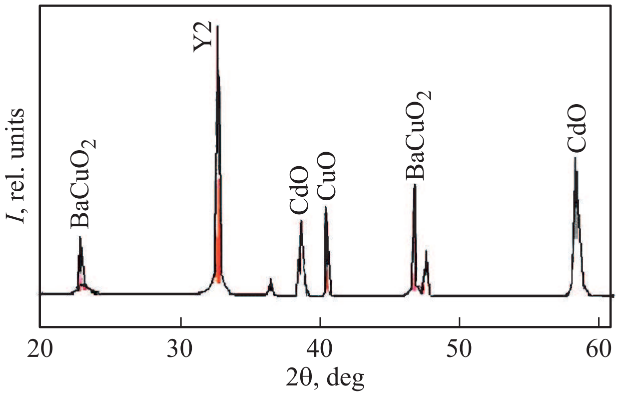

Figure 1. Sample X-ray diffraction pattern $Y_{0.5}Cd_{0.5}Ba_2Cu_3O_{7-\delta}$.

due to the ion valence of yttrium and cadmium, as well as the closeness of their ionic radii (0.90 and 0.95 Å respectively).

Polycrystalline $YBa_2Cu_3O_{7-\delta}$ and $Y_{0.5}Cd_{0.5}Ba_2Cu_3O_{7-\delta}$ were obtained by the method tested in [23,28]. At the first stage, the initial components in a stoichiometric ratio were mixed and annealed in air at a temperature of 1120 K for 25 h. At the second stage, the resulting compositions were annealed in an oxygen atmosphere (at a pressure of 1.2–15 atm) at a temperature of 1190 K for 25 h, then subjected to slow cooling to room temperature. It has been established that when up to 50% of yttrium is replaced by cadmium in the $YBa_2Cu_3O_{7-\delta}$ composition, the superconducting transition is retained at $T_c \sim 84.6$ K.

Samples $8 \times 4 \times 3$ mm were cut from pressed pellets (12 in diameter, 3 mm thick) of synthesized polycrystals. The electrical resistance was measured using a standard four-probe scheme. Current contacts were created by applying a silver paste followed by connecting silver wires 0.05ṁm in diameter to the ends of the polycrystal to ensure uniform current flow over the sample. Potential contacts were also created, which were located on the surface of the sample in its middle part. Then, a three-hour annealing was carried out at a temperature of 200°C in an oxygen atmosphere. Such a procedure allowed to obtain contact resistance less than 1 Ω and to carry out resistive measurements at transport currents up to 10 mA in ab-plane.

In order to study the composition of the resulting $Y_{0.5}Cd_{0.5}Ba_2Cu_3O_{7-\delta}$ HTSC material was subjected to X-ray diffraction analysis. The research result is shown in Fig. 1.

X-ray diffraction analysis showed that, in addition to the main material $Y_{0.5}Cd_{0.5}Ba_2Cu_3O_{7-\delta}$, BaO_2 oxides also exist in X-rays, $BaCuO_2$ and CdO. However, we note that in different compositions of SC polycrystals, in addition to the main crystalline granules, there are always various oxides.

We believe that the difference between the ionic radii of Y and Cd leads to a distortion of the crystal structure of YBCO. This leads to the formation of defects in the structure and the appearance of pinnings in the crystal structure. The resulting pinnings reduce the probability of splitting of superconducting pairs and create the opportunity of a transition to the superconducting state of an HTSC material with a high resistance value in the normal phase.

3. Results and discussion thereof

3.1. Resistive properties

Figure 2 shows the temperature dependences of the resistivity $\rho(T) = \rho_{ab}(T)$ of the $YBa_2Cu_3O_{7-\delta}$ (a) and $Y_{0.5}Cd_{0.5}Ba_2Cu_3O_{7-\delta}$ (b).

Temperature dependence of resistivity of $YBa_2Cu_3O_{7-\delta}$ and $Y_{0.5}Cd_{0.5}Ba_2Cu_3O_{7-\delta}$ samples in the normal phase is well extrapolated by the expression $\rho_n(T) = \rho_0 + kT + BT^2$ (here B and k are some constants (for Y1: $\rho_0 = 18.37\,\mu\Omega \cdot$ cm, $B = 0.000227$ and $k = 0.08$; and for Y2: $\rho_0 = 451.6\,\mu\Omega \cdot$ cm, $B = 0.00175$ and $k = 0.8$)).

Note that the contribution of the quadratic term is much less than the contribution of the linear component, so that the dependence $\rho_n(T)$ can practically be considered linear.

This dependence of the resistivity of the Y1 and Y2 samples, extrapolated to the low temperature region, was used to determine the excess conductivity $\Delta\sigma(T)$ according to

$$\Delta\sigma(T) = \rho^{-1}(T) - \rho_n^{-1}(T). \quad (1)$$

As can be seen in Fig. 2, the value of the critical temperature of samples of the YBaCuO system upon doping with Cd in the considered case remains close to ~ 85 K. In this case, the resistivity $\rho(T)$ of the sample Y2 in the normal phase at 300 K, compared to $YBa_2Cu_3O_{7-\delta}$ increases approximately by 14 times (Table 1).

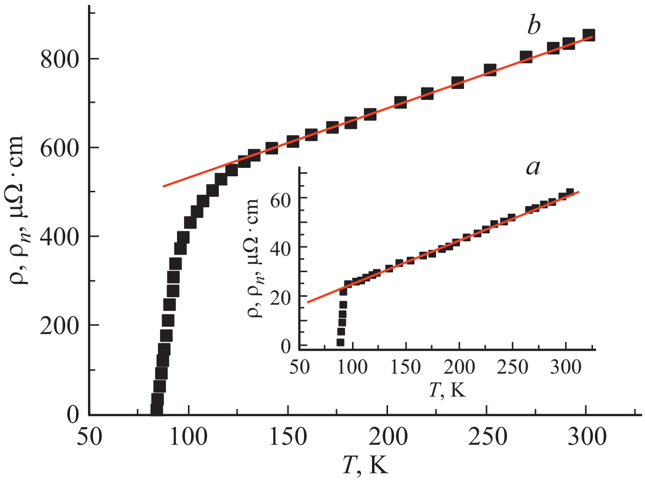

Figure 2. Temperature dependences of resistivity ρ of samples: a — $YBa_2Cu_3O_{7-\delta}$ (Y1) [33] and b — $Y_{0.5}Cd_{0.5}Ba_2Cu_3O_{7-\delta}$ (Y2). The straight lines represent the $\rho_n(T)$ dependences extrapolated to the low temperature region.

Table 1. Sample $Y_{0.5}Cd_{0.5}Ba_2Cu_3O_{7-\delta}$ and $YBa_2Cu_3O_{7-\delta}$ parameters obtained from fluctuation conductivity analysis

YBCO (Cd)	ρ (300 K), $\mu\Omega\cdot$cm	ρ (100 K), $\mu\Omega\cdot$cm	T_c, K	T_c^{mf}, K	T_{G}, K	T_0, K	$\xi_c(0)$, Å	References
Y1 ($x = 0$)	60	24	90.2	91.99	92.1	92.8	1.1	[33]
Y2 ($x = 0.5$)	847	423	84.6	87.1	88	89.6	3.51	–

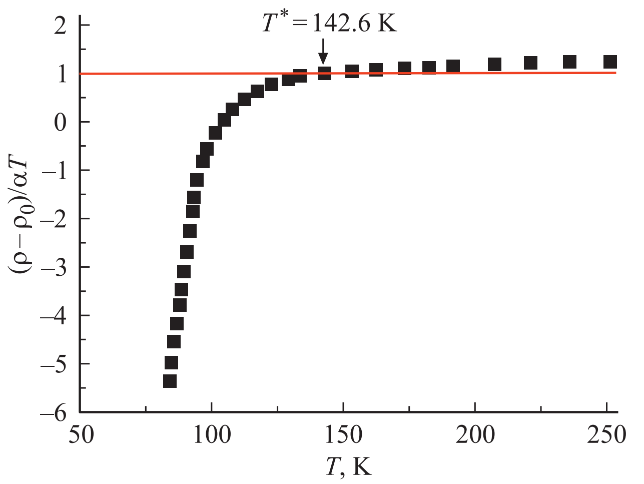

Figure 3. Method for determining T^* sample $Y_{0.5}Cd_{0.5}Ba_2Cu_3O_{7-\delta}$ by criterion $[\rho(T){-}\rho_0]/aT = 1$.

In the temperature range above $T^* = (142.2 \pm 0.5)$ K to 300 K, the dependence $\rho(T)$ of the doped sample Y2 is linear with a slope $d\rho/dT = 0.38\,\mu\Omega\cdot$cm/K (Fig. 1, *b*). A more precise method for determining T^* is based on using the criterion $[\rho(T){-}\rho_0]/aT = 1$, which is obtained by transforming the equation by a straight line [38], where ρ_0 — residual resistance cut off by this line on the y-axis at $T = 0$ K. In this case T^* is defined as the temperature of the deviation of $\rho(T)$ from 1 [32,38] (Fig. 3).

3.2. Analysis of fluctuation conductivity

The fluctuation conductivity in the studied samples was determined from the analysis of the excess conductivity $\Delta\sigma(T)$ by the difference between the measured resistance $\rho(T)$ and the linear normal resistance of the sample $\rho_n(T) = aT + \rho_0$, extrapolated to low temperature region [11,39–42]. Obviously, the excess conductivity $\Delta\sigma(T)$ found in this case, determined by equation (1), should contain information on the temperature dependence of both the FLC and the PG [11,32,39–42].

In order to determine the FLP as part of the local pair (LP) [11,39] model, first of all, it is required to determine the critical temperature in the mean field approximation, which separates the FLP region from the region of critical fluctuations [11,43], i.e. fluctuations of the SP order parameter Δ_0 immediately near T_c (where $\Delta_0 < k_{\mathrm{B}}T$) not taken into account in the Ginzburg–Landau [43] theory. T_c^{mf} — is an important parameter for both FLP and PG analysis, since it determines the reduced temperature

$$\varepsilon = (T/T_c^{\mathrm{mf}} - 1), \tag{2}$$

which is included in all equations of this work.

The method for determining T_c^{mf} for the sample Y2 based on the analysis of the temperature dependence is shown in Fig. 4.

According to Fig. 4, the temperature T_c of the SC transition, T_{G} — the Ginzburg temperature, up to which the mean field theory is valid with decreasing temperatures [44,45] and T_0 — 3D–2D crossover temperature limiting the region of 3D–AL fluctuations from above [35,46].

The fluctuation conductivity for the studied samples was determined by equation (1).

In the works [11,39,42] it is shown that the linear temperature dependence of the resistance in the high temperature region — is a distinctive feature of the normal state of HTSC cuprates, which is characterized by the stability of the Fermi surface [42]. Below the opening temperature of the PG, the Fermi surface is likely to be rearranged [8,42]. As a result, at $T \le T^*$, not only almost all properties of HTSC change and the dependence $\rho(T)$ deviates from the linear dependence [7,39–42], but the carrier density also decreases charge at the Fermi level [47,48], which, by definition, is called a pseudogap [1,7–12]. It is obvious that the excess conductivity $\Delta\sigma(T)$ arising in

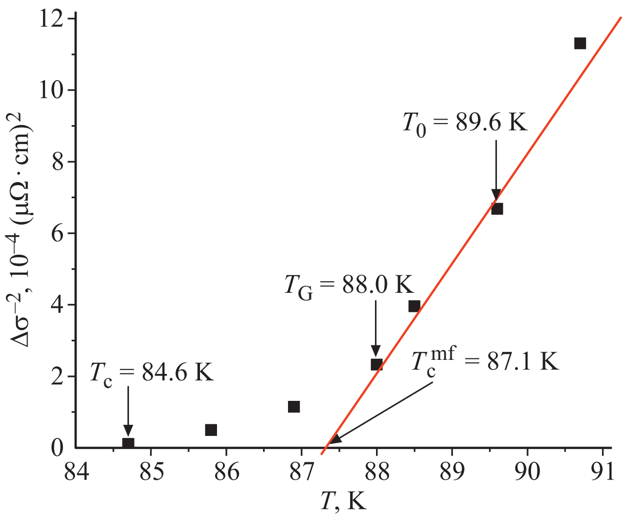

Figure 4. Temperature dependence of the inverse square of the excess conductivity $\Delta\sigma^{-2}(T)$ of the $Y_{0.5}Cd_{0.5}Ba_2Cu_3O_y$ polycrystal, which determines T_c^{mf} of pattern Y2. The arrows indicate the characteristic temperatures T_c, T_{G} and T_0.

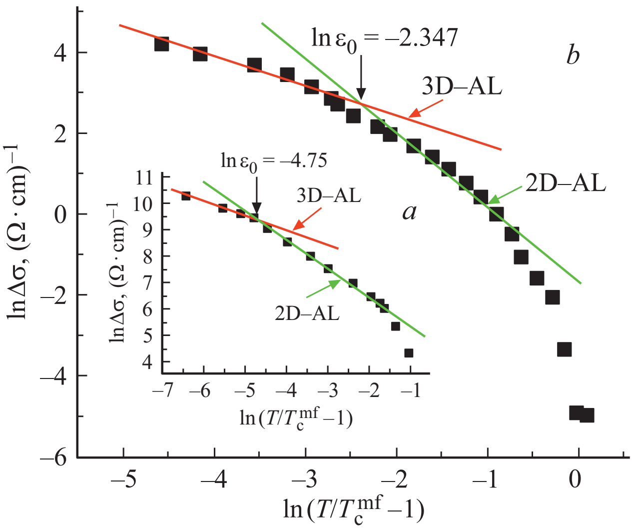

Figure 5. Dependences of logarithm of excess conductivity from $\ln(T/T_c-1)$ of samples Y1 [33] and Y2. Solid lines — calculation as part of the Aslamazov–Larkin theory.

this case, determined by equation (1), should contain information about the temperature dependence of both FLP and PG [11,32,39–42]. This approach was used to analyze the $\Delta\sigma(T)$ sample Y1.

In HTSC near T_c, the coherence length along the c axis is greater than the corresponding YBCO lattice cell size $d = c = 11.7$ Å [33], and fluctuation superconducting pairs (FSCP) interact in the entire volume of the superconductor. Accordingly, this is the region of 3D fluctuations. As a result, up to the temperature of the 3D–2D crossover $T_0 > T_c^{mf}$, the $\Delta\sigma(\varepsilon)$ conductivity is always extrapolated by the fluctuation contribution of the Aslamazov–Larkin theory [34] for 3D systems [11,39–41]:

$$\Delta\sigma_{\mathrm{AL3D}} = C_{\mathrm{3D}}\{e^2/[32\hbar\xi_c(0)]\}\varepsilon^{-1/2}. \tag{3}$$

Hence it easily follows that $\Delta\sigma^{-2}(T) \sim \varepsilon \sim (T - T_c^{mf})$. As shown in Fig. 3, for sample Y2, the extrapolated linear dependence $\Delta\sigma^{-2}(T)$ goes to zero at $T = T_c^{mf}$ [(46)43]. Having determined T_c^{mf}, it is possible to construct the dependence of $\ln\Delta\sigma$ on $\ln\varepsilon$ for samples Y1 and (Fig. 4).

It can be seen from Fig. 5 that, near T_c, the FLC in all cases is well approximated by the fluctuation contribution of AL for 3D systems (3) (straight 3D–AL lines with slope $\lambda = -1/2$). This means that the classical 3D FLC is always realized in cuprate HTSC when T tends to T_c and $\xi_c(T) > d$ [11,32,39,41]. Above T_0, the dependence of $\ln\Delta\sigma$ on $\ln\varepsilon$ sharply changes the slope. Such dependence with slope $\lambda = -1$ is typical for 2D–AL fluctuations [34]:

$$\Delta\sigma_{\mathrm{AL2D}} = C_{\mathrm{2D}}\{e^2/[16\hbar d]\}\varepsilon^{-1}. \tag{4}$$

Thus, at a T_0 temperature, the value of which is given in Table 1, a 3D–2D crossover occurs. It is obvious that $\xi_c(T_0) = d$, whence we obtain

$$\xi_c(0) = d\sqrt{\varepsilon_0}. \tag{5}$$

3.3. Analysis of the magnitude and temperature dependence of the pseudogap

As noted above, in cuprates at $T < T^*$, the density of electronic states of quasiparticles decreases at the Fermi level [12,47–49] (the reason for this phenomenon has not yet been fully elucidated), which creates conditions for the formation of a pseudogap in excitation spectrum [10–12,44] and ultimately leads to the formation of excess conductivity. The magnitude and temperature dependence of the pseudogap in the studied samples were analyzed as part of the LP model [11,50] taking into account the theory [51–53] predicted for HTSC for the transition from Bose-Einstein condensation (BEC) to the BCS regime as the temperature decreases in the interval $T^* < T < T_c$. Note that excess conductivity exists precisely in this temperature range, where fermions presumably form pairs — the so-called strongly-coupled bosons (SCB) [10,11,51–53]. The pseudogap is characterized by a certain value the binding energy $\varepsilon_b \sim 1/\xi^2(T)$, which causes the creation of such pairs [51–53], which decreases with temperature, since the coherence length of superconducting pairs $\xi(T) = \xi(0)(T/T_c-1)^{-1/2}$, on the contrary, increases as T [40] decreases. Therefore, according to the LP model, SCB transform into FSCP as T approaches T_c (BEC–BCS transition), which becomes possible due to the exceptionally small coherence length $\xi(T)$ in cuprates [11,42,54–56].

Our studies allow to estimate the magnitude and temperature dependence of PG, based on the temperature dependence of excess conductivity over the entire temperature range from T^* to T_c according to [11,50,56]:

$$\Delta\sigma(\varepsilon) = \left\{\frac{A(2 - T/T^*)[\exp(-\Delta^*/T)]e^2}{16\hbar\xi_c(0)\sqrt{2\varepsilon_0^*\,\mathrm{sh}(2\varepsilon/\varepsilon_0^*)}}\right\}, \tag{6}$$

where $(1 - T/T^*)$ determines the number of pairs formed at $T \le T^*$: a $\exp(-\Delta^*/T)$ — the number of pairs destroyed by thermal fluctuations below the BEC–BCS transition temperature. The factor A has the same meaning as the factors C_{3D} and C_{2D} in equations (3) and (4).

The solution of equation (6) gives the value Δ^*:

$$\Delta^*(T) = T\ln\left\{\frac{A(1 - T/T^*)e^2}{\Delta\sigma(T)16\hbar\xi_c(0)\sqrt{2\varepsilon_0^*\,\mathrm{sh}(2\varepsilon/\varepsilon_0^*)}}\right\}, \tag{7}$$

where $\Delta\sigma(T)$ — excess conductivity determined in the experiment.

Figure 6 shows the dependences of the logarithm of the excess conductivity of the sample Y2 on the reciprocal temperature. The choice of such coordinates is due to the strong sensitivity of the linear segment $\ln\Delta\sigma(1/T)$ to the value $\Delta^*(T_c)$ in equation (6), which allows to estimate this parameter with high accuracy (this needed to find the factor A) [11,(49)50,57]. It was also shown in the works [1,32,39] that in these coordinates the shape of the theoretical curve turned out to be very sensitive to the value of $\Delta^*(T_{\mathrm{G}})$. The dependences

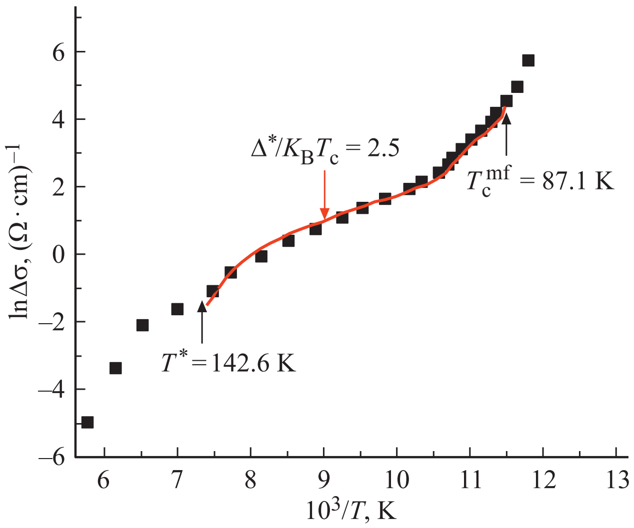

Figure 6. Dependences of the logarithm of the excess conductivity on the reciprocal temperature of the polycrystal $Y_{0.5}Cd_{0.5}Ba_2Cu_3O_{7-\delta}$, solid lines — approximation of the equation (6) with the parameters given in the text.

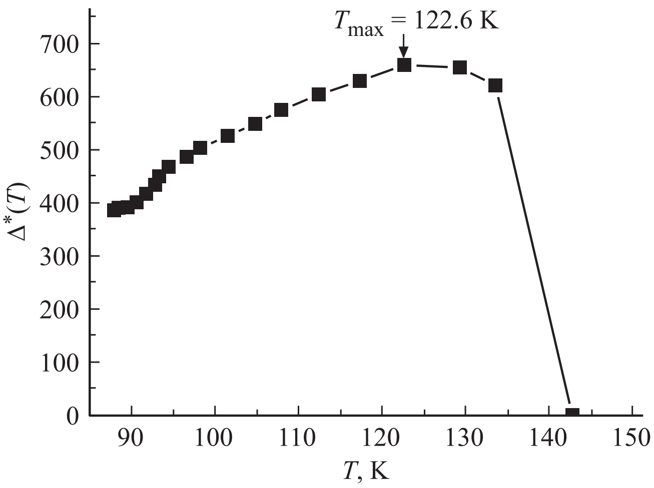

Figure 7. Temperature dependences of the calculated value of the sample pseudogap Y2 with the parameters given in the text. The arrows show the maximum values of the pseudogap.

$\ln\Delta\sigma(1/T)$ were calculated according to the method tested in [20,58]. In addition, it is assumed that $\Delta^*(T_G) = \Delta_0(0)$, where Δ_0 — SG gap [55,56]. Let's underline that it is the value $\Delta^*(T_G)$ that determines the true value of the PG and is used to estimate the value of the BCS ratio $D^* = 2\Delta_0(0)/K_BT_c = 2\Delta^*(T_G)/K_BT_c$ in a specific HTSC sample [1,32,39]. The best approximation of the dependence of $\ln\Delta\sigma$ on $1/T$ by equation (6) for sample Y2 is achieved at $D^* = 5 \pm 0.2$.

Equations (6) and (7) include a number of parameters, which are also determined from experiment within the framework of the LP model [32,40]. In addition to T_c, $\xi_c(0)$ and ε, which are obtained from resistive measurements

Table 2. Parameter of pseudogap analysis of HTSC material $Y_{0.5}Cd_{0.5}Ba_2Cu_3O_{7-\delta}$

YBCO (Cd)	T^*, K	A^*	T_m, K	D^*, K	$\Delta^*(T_m)$, K	$\Delta^*(T_G)$, K
Y2 ($x = 0.5$)	142.6	16.6	122.6	2.5	660	385

and FLP analysis, both equations include a factor A, which has the same meaning as C-factor in FLP theory, and theoretical parameter ε_0^* [49–51]. According to [59,60], the optimal approximation for HTSC material is achieved at $2\Delta^*(T)/k_BT \approx 5-7$. For sample Y2, the value is $2\Delta^*(T_c)/k_BT_c = 5$. As a result, from the LP analysis for sample Y2, values A equal to 16.6 were obtained.

Based on the obtained sample parameter Y2, the dependences $\Delta\sigma(\varepsilon)$ were calculated using equation (7) and, comparing theory with experiment in the region of 3D−AL fluctuations near T_c, where $\ln\Delta\sigma(\ln\varepsilon)$ — linear function of reduced temperature ε with slope $\lambda = -1/2$ [32,40,59] good agreement of equation (6) with experiment in the temperature range from T^* to T_G. This feature belongs to one of the main properties of most HTSC [11,40,49–51]. It can be assumed that equation (7) gives reliable values of the value and temperature dependence of PG.

The temperature dependence and the value of the pseudogap parameter $\Delta^*(T)$ (Fig. 6) were calculated on the basis of equation (7) with the parameters given in Tables 1 and 2. As noted in [11,48], the value of the factor A is selected from the condition of the coincidence of the temperature dependence $\Delta\sigma$ (eq. 6), setting $\Delta^* = \Delta^*(T)$ with experimental data in the region 3D of fluctuations near T_c.

It is also seen from the data presented in Fig. 7 that, with decreasing temperature, the magnitude of the pseudogap first increases, then, after passing through a maximum, decreases. This decrease is due to the transformation of the SCB into the FSCP as a result of the BEC−BCS transition, which is accompanied by an increase in the excess conductivity at $T \to T_c$. This behavior Δ^* with decreasing temperature was first observed on YBCO [11,48] films with different oxygen contents, which is apparently typical of cuprate HTSC [51].

4. Conclusion

Thus, it can be concluded that, in the $Y_{0.5}Cd_{0.5}Ba_2Cu_3O_{7-\delta}$ we studied, the formation of local pairs of carriers charge at $T \gg T_c$, which creates conditions for the formation of a pseudogap [10–12] with the subsequent establishment of phase coherence of fluctuation superconducting pairs at $T < T_c$ [59,60].

The study showed that near T_c the fluctuation conductivity is well described in terms of the Aslamazov−Larkin fluctuation theory: 3D−AL. Above the 3D−2D crossover temperature, the 2D−AL theory is applicable.

Conflict of interest

The authors declare that they have no conflict of interest.

References

[1] R.V. Vovk, A.L. Soloviev. Low Temp. Phys. **44**, 81 (2018).
[2] R.J. Cava. Science **243**, 656 (1990).
[3] M. Asta, D. de Futaine, G. Ceder, E. Salomons, M. Kraitchman. J. Less. Common. Metals **168**, 39 (1991).
[4] R.V. Vovk, N.R. Vovk, O.V. Dobrovolskiy. J. Low Temp. Phys. **175**, 614 (2014).
[5] R.V. Vovk, Z.F. Nazyrov, M.A. Obolenskii, I.L. Goulatis, A. Chroneos, V.M. Pinto Simoes. J. Alloys Compd. **509**, 4553 (2011).
[6] S.V. Savich, A.V. Samoilov, R.V. Vovk, O.V. Dobrovolskiy, S.N. Kamchatna, Ya.V. Dolgopolova, O.A. Chernovol-Tkachenko. Mod. Phys. Lett. B **30**, 1650034 (2016).
[7] T. Timusk, B. Statt. Rep. Prog. Phys. **62**, 61 (1999).
[8] S. Badoux, W. Tabis, F. Laliberte, G. Grissonnanche, B. Vignolle, D. Vignolles, J. Beard, D.A. Bonn, W.N. Hardy, R. Liang, N. Doiron-Leyraud, Louis Taillefer, Cyril Proust. Nature (London) **531**, 210 (2016).
[9] Rui-Hua He, M. Hashimoto, H. Karapetyan, J.D. Koralek, J.P. Hinton, J.P. Testaud, V. Nathan, Y. Yoshida, Hong Yao, K. Tanaka, W. Meevasana, R.G. Moore, D.H. Lu, S.-K. Mo, M. Ishikado, H. Eisaki, Z. Hussain, T.P. Devereaux, S.A. Kivelson, J. Orenstein, A. Kapitulnik, Z.-X. Shen. Science **331**, 1579 (2011).
[10] R. Peters, J. Bauer. Phys. Rev. B **92**, 014511 (2016).
[11] A.L. Solovjov. Superconductors — Material. Properties and Applications. Ch. 7. Pseudogap and Local Pairs in High-Tc Superconductors / Ed. A.M. Gabovich. Rijeka: InTech (2012). 137 p.
[12] A.A. Kordyuk. Fiz. Nizk. Temp. **41**, 417 (2015). [Low Temp. Phys. **41**, 319 (2015)].
[13] T. Suzuki, T. Yamazaki, R. Sekine. J. Mater. Sci. Lett. **8**, 381 (1989).
[14] V.N. Narozhnyi, V.N. Kochetkov. Phys. Rev. B **53**, 5856 (1996).
[15] M. Murakami, N. Sakai, T. Higuchi. Supercond. Sci. Technol. **12**, 1015 (1996).
[16] A.L. Soloviev, V.M. Dmitriev. Low Temp. Phys. **33**, 23 (2007).
[17] R.V. Vovk, M.A. Obolensky, A.A. Zavgorodniy, A.V. Bondarenko, M.G. Revyakin. Low Temp. Phys. **33**, 408 (2007).
[18] L.P. Kozeev, M.Yu. Kamenev, A.I. Romanenko, O.B. Anikeeva, V.E. Fedorov. Mater. VI Intern. conf. „Crystals: growth, properties, real structure, applications“ (8–12 September 2003). VNIISIMS Publishing House (2003). (in Russian).
[19] E.V. Yakubovich, N.N. Oleynikov, V.A. Ketsko, I.V. Arkhangelsky. Dokl. RAS **386**, 502 (2002).
[20] S. Kambe, G. Samukama, K. Yamaguchi, O. Ishu, I. Shime, T. Nomura, S. Ohshima, K. Okuyama, T. Itoh, H. Suematsu, H. Yamauchi. Solid State Phys. **108**, 283 (1998).
[21] J.W. Chen, C.F. Chen. Solid State Commun. **69**, 1079 (1989).
[22] N.E. Alekseevskii, A.V. Mitin, V.I. Nizhankovsky, E.P. Khlybov, V.V. Evdokimova, G.M. Kuzmichev. SFKhT **2**, 40 (1989). (in Russian).
[23] S.A. Aliev, J.A. Baghirov, S.S. Ragimov, S.A. Huseyhov, V.M. Aliev, I.A. Ismailov, A.Sh. Mechtiev. Proc. 2nd Int. Conf. on Rare Earth Development and Application. Beijing, China (1991).
[24] R.V. Vovk, Z.F. Nazyrov, M.A. Obolenskii, V.M. Pinto Simoes, M. Januszczyk, J.N. Latosińska. Acta Phys. Polonica A **120**, 512 (2011).
[25] V.M. Aliev. Transact. Azerbaijan Nat. Academy Sci. Phys. Astronomy **32**, *2*, 110 (2012).
[26] V.M. Aliev, S.S. Ragimov, R.I. Selimzade. Low Temp. Phys. **39**, 493 (2013).
[27] S.A. Aliev, S.S. Ragimov, V.M. Aliev. Azerbaijan J. Phys. **10**, *4*, 42 (2004).
[28] V.M. Aliev, S.A. Aliev, S.S. Ragimov, G.J. Sultanov, B.A. Tairov. Low Temp. Phys. **37**, 273 (2011).
[29] Yu.D. Tretyakov, E.A. Gudilin. UFN, **69**, 1 (2000). (in Russian).
[30] E.A. Gudilin, A.P. Soloshenko, V.V. Lennikov, A.V. Knotko, D.A. Vetoshkin, N.N. Oleynikov, Yu.D. Tretyakov. ZhNKh **45**, 917 (2000) (in Russian).
[31] R. Fehrenbacher, T.M. Rice. Phys. Rev. Lett. **70**, 3471 (1993).
[32] A.L. Soloviev, L.V. Omelchenko, R.V. Vovk, S.N. Kamchatnaya. Low Temp. Phys. **43**, 841 (2017).
[33] V.M. Aliev, R.I. Selimzade, J.A. Ragimov, L.V. Omelchenko, E.V. Petrenko. FTT **46**, *9*, 1068 (2020). (in Russian).
[34] L.G. Aslamazov, A.I. Larkin. Phys. Lett. A **26**, 238 (1968).
[35] S. Hikami, A.I. Larkin. Mod. Phys. Lett. B **2**, 693 (1988).
[36] M. Randeria. Nat. Phys. **6**, 561 (2010).
[37] I. Esterlis, S.A. Kivelson, D.J. Scalapino. Phys. Rev. B **99**, 174516 (2019).
[38] E.V.L. de Mello, M.T.D. Orlando, J.L. Gonzalez, E.S. Caixeiro, E. Baggio-Saitovich. Phys. Rev. B **66**, 092504 (2002).
[39] A.L. Solovjov, L.V. Omelchenko, V.B. Stepanov, R.V. Vovk, H.-U. Habermeier, H. Lochmajer, P. Przyslupski, K. Rogacki. Phys. Rev. B **94**, 224505 (2016).
[40] M.S. Grbić, M. Požek, D. Paar, V. Hinkov, M. Raichle, D. Haug, B. Keimer, N. Barčić, A. Dulčić. Phys. Rev. B **83**, 144508 (2011).
[41] W. Lang, G. Heine, W. Kula, R. Sobolewski. Phys. Rev. B **51**, 9180 (1995).
[42] B.P. Stojkovic, D. Pines. Phys. Rev. B **55**, 8576 (1997).
[43] B. Oh, K. Char, A.D. Kent, M. Naito, M.R. Beasley, T.H. Geballe, R.H. Hammond, J.M. Graybeal, A. Kapitulnik. Phys. Rev. B **37**, 7861 (1988).
[44] P.G. De Gennes. Superconductivity of Metals and Alloys, W.A. Benjamin. INC., N.Y.–Amsterdam (1966). 280 p.
[45] A. Kapitulnik, M.R. Beasley, C. Castellani, C. Di Castro. Phys. Rev. B **37**, 537 (1988).
[46] Y.B. Xie. Phys. Rev. B **46**, 13997 (1992).
[47] A.I. Dyachenko, V.Yu. Tarenkov, S.L. Sidorov, V.N. Varyukhin, A.L. Soloviev. FNT **39**, 416 (2013). (in Russian).
[48] H. Alloul, T. Ohno, P. Mendels. Phys. Rev. Lett. **63**, *16*, 1700 (1989).
[49] T. Kondo, A.D. Palczewsk, Y. Hamaya, T. Takeuchi, J.S. Wen, Z.J. Xu, G. Gu, A. Kaminski. Phys. Rev. Lett. **111**, 157003 (2013).
[50] R.F. Trunin. UFN **175**, *10*, 1017 (2005). (in Russian).
[51] V.M. Loktev. Low Temp. Phys. **22**, 488 (1996).
[52] R. Haussmann. Phys. Rev. B **49**, 12975 (1994).
[53] J.R. Engelbrecht, A. Nazarenko, M. Randeria, E. Dagotto. Phys. Rev. B **57**, 13406 (1998).

[54] T. Ito, K. Takenaka, S. Uchida. Phys. Rev. Lett., **70**, *25*, 3995 (1993).
[55] The Physics of Superconductors. V. 1. Conventional and High-Tc superconductors / Ed. K.H. Bennemann, J.B. Katterson. Springer, Berlin (2003). 966 p.
[56] B. Leridon, A. Défossez, J. Dumont, J. Lesueur, J.P. Contour. Phys. Rev. Lett. **87**, 197007 (2001).
[57] D.D. Prokofiev, M.P. Volkov, Yu.A. Boikov. FTT **45**, 1168 (2003). (in Russian).
[58] D.S. Inosov, J.T. Park, A. Charnukha, Yuan Li, A.V. Boris, B. Keimer, V. Hinkov. Phys. Rev. B **83**, 214520 (2011).
[59] V.V. Florentiev, A.V. Inyushkin, A.I. Taldenkov, O.K. Melnikov, A.B. Bykov. SFKhT **3**, *10*, 2 (1990). (in Russian).
[60] Ya. Ponomarev, M. Mikheev, M. Sudakova, S. Tchesnokov, S. Kuzmichev. Phys. Status Solidi C **6**, 2072 (2009).

Translated by E.Potapova